Variable Time Lag and Backward Ejection in Full-Dimensional Analysis of Strong-Field Double Ionization

S. L. Haan,[1,*] L. Breen,[1] A. Karim,[1] and J. H. Eberly[2,†]
[1]*Department of Physics and Astronomy, Calvin College, Grand Rapids Michigan 49546, USA*
[2]*Department of Physics and Astronomy, University of Rochester, Rochester, New York 14627, USA*
(Received 6 April 2006; published 8 September 2006)

Ensembles of 400 000 two-electron trajectories in three space dimensions are used with Newtonian equations of motion to track atomic double ionization under very strong laser fields. We report a variable time lag between *e*-*e* collision and double ionization, and find that the time lag plays a key role in the emergence directions of the electrons. These are precursors to production of electron momentum distributions showing substantial new agreement with experimental data.

DOI: 10.1103/PhysRevLett.97.103008 PACS numbers: 32.80.Rm, 32.60.+i

Data from nonsequential double ionization (NSDI) of atoms by short intense laser pulses are of unusual interest in strong-field atomic physics because they reveal very highly correlated electron-electron behavior. A generally accepted view is that ionization of the second electron occurs after the first electron has traveled out from the core and then is returned by the laser field for an energy-transferring ''recollision'' with the second electron [1]. One thus might expect, and the main body of theoretical analysis to date has suggested, that after recollision most ionized electron pairs should emerge together in the same momentum hemisphere [2,3] relative to the axis of laser polarization. However, experiments with He [4,5] and other noble gas atoms [6–8] using cold target recoil ion momentum spectroscopy (COLTRIMS) [8,9] find substantial numbers of opposite-hemisphere ejections as well. This discrepancy between theory and experiment has proven difficult to overcome.

In the present Letter we show that a treatment permitting a continuous-time 3D examination can resolve the conflict. Working with large statistical ensembles of classical electron pairs as surrogates for inaccessible quantum probabilities, we find that significantly many opposite-hemisphere as well as same-hemisphere emissions occur, as shown in Fig. 1, with ranges of momenta that are now in basic agreement with experiment. Same-hemisphere trajectories appear in quadrants 1 and 3, and opposite-hemisphere trajectories appear in quadrants 2 and 4.

Our treatment is, of course, not a suggestion that classical physics describes atoms, but that in the presence of the strong laser force the electrons are in a classical regime much of the time where the laser field's phasing is important [10]. Additionally, a classical analysis has important strengths: (i) the entire process of double ionization, in which both electrons are allowed to interact smoothly and continuously with each other, with the nuclear charge, and with the laser field, can be easily calculated from beginning to end of the laser pulse, and (ii) after the pulse, or at any time, individual double-ionization trajectories can be back analyzed to extract insights from their histories [11].

These advantages have been utilized in classical strong-field studies before and their successes [11] toward understanding NSDI have motivated the present work. However, the previous studies have worked almost exclusively within the so-called aligned-electron approximation [12], in which the electron motion is confined to the laser's polarization axis where most of the high-field response is expected to lie. Here we report the first momentum results obtained in a fully 3D classical treatment. We find that an opposite-hemisphere pattern of final momenta comes from a previously unanalyzed time lag that occurs between the recollision time and the time of the double ionization. This time lag is absent from quantum calculations made so far [2,13] and it may underlie their difficulty in explaining contributions to the opposite-hemisphere momentum distributions.

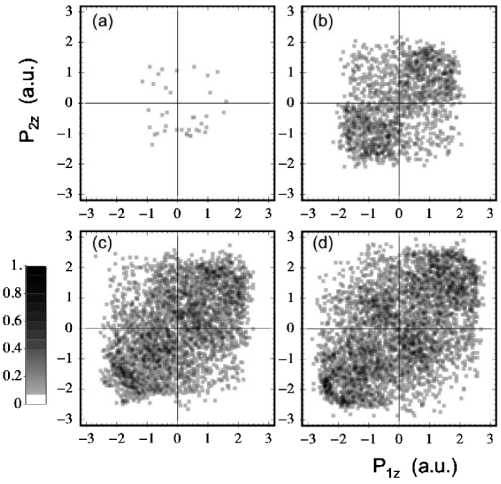

FIG. 1. Scatter plot of final momenta along the laser polarization axis, p_{2z} vs p_{1z}, for doubly ionized electron pairs. Laser intensities for parts (a)–(d) are 2, 4, 6, and 8×10^{14} W/cm^2, respectively. Each electron's momentum has maximum of about $(4U_p)^{1/2}$—1.3, 1.8, 2.2, and 2.6 a.u., respectively. There are no points outside our plotting area. To our knowledge, these results are the first to be in basic agreement with experiment [4] in all four quadrants.

The classical-ensemble method that we use has been described previously for the aligned-electron model (Panfili, *et al.* [11], and see [14] for the 3D analog). The infinitely deep Coulomb potential of the nucleus could pose a challenge because it can make a classical multielectron model unstable against autoionization [15]. However, the familiar soft core of 1D analysis eliminates this—in 3D one replaces $-2/r$ with $-2/(r^2 + a^2)^{1/2}$. If the initial combined energy of the electrons is set to the energy of the helium ground state, -2.9035 a.u., then a shielding value $a > 0.69$ a.u. ensures stability in three dimensions. The present results come from calculations where we set $a = 0.825$ a.u. and employed a shielding parameter 0.05 a.u. for the electron-electron interaction. We used a nearly 15 fs pulse (10-cycle trapezoidal shape with 2-cycle on and off ramps and 6 cycles full strength), linearly polarized in the z direction. We chose the common experimental wavelength 780 nm (angular frequency $\omega = 0.0584$ a.u.), corresponding to 16-photon single ionization and 50-photon double ionization of helium.

The scatter plots in Fig. 1 include all our NSDI trajectories. We did not symmetrize our results, so all symmetry about the line $p_{2z} = p_{1z}$ arises from the dynamics itself. The nearly sharp cutoff of the point distribution indicates a definite range for each electron's momentum, independent of the other electron's momentum. Each electron can have momentum up to about $(4U_p)^{1/2}$, the peak drift momentum for an individual electron starting from rest in an oscillating electric field. These features are all in accord with experiment.

We can take further advantage of back analysis. At the end of the pulse, if we select the trajectories with doubly ionized pairs, back analysis allows us easily to determine their times of double ionization (DI) and closest collision. We define the time of recollision to be the time of closest approach of the two electrons during the recollision, and the time of double ionization to be the first time when both electrons either have energy greater than zero or are outside the potential energy well that surrounds the nucleus [16]. We have segregated the trajectories already shown in part (c) of Fig. 1 according to the time lag between closest recollision and their times of double ionization, and the results are displayed in Fig. 2. There we show projections of final momenta on the longitudinal direction of the recolliding electron, positive or negative, in each case. Thus, a negative coordinate indicates a final sign for p_z that is opposite from the sign of p_z that the returning electron had just before recollision.

Parts (a)–(d) of the figure show final-momentum projections for trajectories that had time lags from very short (less than 0.04 cycle) to substantial (more than 0.50 cycle). We see in Fig. 2(a) that double ionizations with very little time lag following "hard-hit" recollisions lead to same-hemisphere final momenta. In the three plots (a)–(c), back analysis shows that the momentum projections are largely

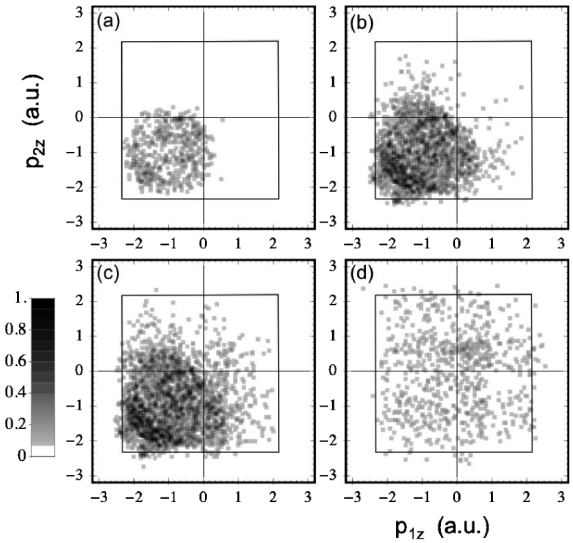

FIG. 2. Scatter plots of p_{2z} vs p_{1z} for laser intensity 6×10^{14} W/cm^2, filtered for time delay between closest recollision and ionization, and projected onto the direction of return ($\pm z$) of the recolliding electron. Population in the third quadrant thus indicates final drift momenta in the opposite momentum hemisphere from the direction of impact in the closest recollision. Maximum time lags for parts (a)–(c) are 1/25, 1/4, and 1/2 laser cycle, respectively. Part (d) shows trajectories for which the time lag is greater than 1/2 laser cycle. Interior boxes show $\pm(4U_p)^{1/2}$.

negative. This means that by far the most common situation is that double-electron ejection occurs in the backward direction, compared to the recolliding impact direction.

In parts (b) and (c) of Fig. 2 we see that for increased time lag there is also increased spillover into the second and fourth quadrants (opposite-hemisphere ejections). Finally, part (d) complements (c) and shows all trajectories with lags greater than 0.50 cycle. These last trajectories are well distributed, as would be expected for uncorrelated emissions. We conclude from Fig. 2 that the major source of final-state population in opposite hemispheres is double ionization in which there is a time lag between closest recollision and ionization, with time lags of more than 0.04 cycle leading to "spillover" into the opposite hemispheres, and time lags of more than half a cycle leading to uncorrelated emissions.

To report the effect of this time lag more fully, we present in Fig. 3 the total fraction of DI versus time lag for several laser intensities. In the important range 0.4–1.2 PW/cm^2, at most 15% of the DI occurs extremely promptly (within 0.04 cycles of the closest recollision). This result unambiguously shows the importance of a finite delay. However, the delay is not very long because for these intensities over 60% of the DI occurs within one-third cycle of the closest recollision. Thus, the time lag between recollision and double ionization is not the

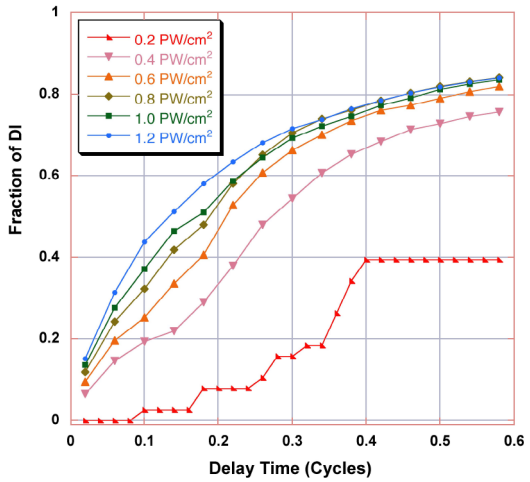

FIG. 3 (color online). Accumulated fraction of double ionization vs time lag between closest recollision and double ionization for the intensities indicated.

multiple-half-cycle time delay that one might expect for recollision excitation with subsequent tunneling ionization [10]. We infer that whatever excited complex is formed in the recollision is usually quenched (i.e., ionized) within less than a half laser cycle. Details of the figure depend on the specific definition of the time of ionization. For example, if we were to require energy greater than zero for an electron to be considered ionized [16], the curves would shift toward longer delay times. For the lowest intensity shown, 0.2 PW/cm^2, ionization typically lags recollision by more than half a cycle. Examination of individual trajectories reveals that for this intensity it is common to have multiple energy-transferring recollisions.

We next consider the laser phase at closest recollision and at double ionization. Part (a) of Fig. 4 shows a histogram of the percentage of DI trajectories vs laser phase at the time of closest recollision. We have divided each laser

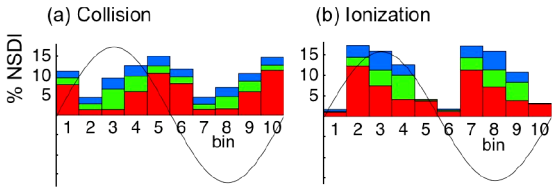

FIG. 4 (color online). Histograms of the percentage of double-ionization trajectories vs laser phase (by bin number) at (a) closest recollision and (b) double ionization. The bottom bands (red) tally trajectories that doubly ionize into the same momentum hemispheres (based on the sign of p_z) within a half cycle of closest recollision. The middle bands (green) represent trajectories that doubly ionize into opposite momentum hemispheres within a half laser cycle, and the top bands (blue) represent trajectories that have a time lag of more than one-half cycle. Laser intensity is 6×10^{14} W/cm^2.

cycle into 10 bins. We treat the first and second half of the cycles separately as a consistency check. The full histogram includes all DI trajectories. The bottom bands (red) denote trajectories that result in final momenta in the same hemisphere (quadrants 1 or 3 in Fig. 1) and that have delay times of 1/2 cycle or less. The intermediate bands (green) represent trajectories that lead to opposite hemispheres, also for maximum time delay of one-half cycle. Finally, the top bands (blue) represent trajectories with delay times of more than half a cycle. We note that the collisions can occur throughout most of the laser cycle, but consistent with the simple-man model [1] they peak slightly before the zeroes of the laser field. Part (b) of the figure shows the phases at final ionization. The phase lag from closest recollision to ionization is clear. It is also evident from the intermediate (green) bands that the majority of the ionization that leads to opposite-hemisphere electrons occurs when the laser field is near or shortly past its peak.

The drift velocity of a particle (in one dimension) exposed only to an oscillatory force $-eE_0 \sin(\omega t)$ is $v_{\pi/2} = v_0 - eE_0/(m\omega)$, where v_0 is its velocity at $t = 0$; $v_{\pi/2}$ is also its velocity at $\omega t = \pi/2$. Thus, after a collision that occurs in the positive z direction and at a field minimum, the higher energy electron will—to first approximation—have postcollision velocity v_0 but drift velocity $v_0 - eE_0/(m\omega)$. Because the electron will have given up a sizable fraction of its energy in the recollision, the latter of the terms will typically have greater magnitude, and the electron will emerge in a direction *opposite* to the impact direction, as in Fig. 2. The maximum speed is then $eE_0/(m\omega) = (4U_p)^{1/2}$, and is attained for $v_0 = 0$. This result differs from what is expected purely on energy considerations (e.g., Refs. [7,8]) since then electrons could emerge with speeds up to $v_0 + eE_0/(m\omega)$. Our results explain why those high-energy electrons have not been observed.

If the second electron is directly ionized by the collision or ionizes before the field peaks, it can be expected to drift out in the same direction as the first electron, opposite from the impact direction. However, if the second electron does not escape until after the field maximum, then (again, to first approximation, and depending on its speed as it escapes) its drift velocity may be reversed compared with the first electron. Thus phase delay between closest recollision and ionization provides a straightforward explanation for the opposite-hemisphere trajectories [17].

In this Letter we have shown that large classical full-dimensional ensembles of NSDI electrons contain substantial numbers of both same-hemisphere and opposite-hemisphere electron emissions, in agreement with experiment. There is further agreement in predicting a nearly sharp electron momentum limit of approximately $(4U_p)^{1/2}$. We have used 3D classical back analysis and sorting to examine large numbers of individual recollision trajectories from laser-pulse turn-on to turn-off. We have found

that immediate impact-recollision ionization accounts for just a small portion of the double ionization, and is accompanied by a reversal of ejection direction. For the greatest fraction of ejections, back analysis reveals a time lag between closest recollision and double ionization, which has a determining effect on the final-momentum distribution. Our data will permit further analysis, e.g., of 3D transverse momenta, which we must defer for lack of space. A 2D transverse classical model is currently providing a fresh visualization of Coulomb focusing [18].

Following the Corkum proposal [1], almost all previous theoretical treatments have included one or more quantum elements, most commonly initiation by single-electron tunneling or a final postcollision tunnel ionization, all of which are now seen to be unnecessary. The view provided here is that classical electron correlation is so strong in the main zone of physical activity that NSDI is unavoidably and essentially not only a two-electron process, but a two-active-electron classical process. The previously unremarked time lag, and its importance in leading to opposite-hemisphere emissions, illustrate an inadequacy of a one-electron view. The ejection direction reversal is qualitatively striking and it also explains quantitatively why the maximum momentum observed is less than what has been calculated from energy considerations alone (e.g., see [7,8]).

This material is based upon work supported by the National Science Foundation under Grant No. 0355035 to Calvin College and by DOE Grant No. DE-FG02-05ER15713 to the University of Rochester. We acknowledge contributions to computer programming by R. Panfili, J. C. Cully, D. Tannor, and A. Vache.

*Electronic address: haan@calvin.edu
†Electronic address: eberly@pas.rochester.edu

[1] P. B. Corkum, Phys. Rev. Lett. **71**, 1994 (1993); see also, K. C. Kulander, K. J. Schafer, and J. L. Krause, in *Super Intense Laser-Atom Physics*, edited by B. Piraux, A. L'Huillier, and K. Rzazewski (Plenum, New York, 1995), p. 95.

[2] For example, S. P. Goreslavskii, S. V. Popruzhenko, R. Kopold, and W. Becker, Phys. Rev. A **64**, 053402 (2001); S. P. Goreslavksii and S. V. Popruzhenko, Opt. Express **8**, 395 (2001); A. Becker and F. H. M. Faisal, Phys. Rev. Lett. **89**, 193003 (2002); C. Figueira de Morisson Faria, H. Schomerus, X. Liu, and W. Becker Phys. Rev. A **69**, 043405 (2004).

[3] J. Chen, J. Liu, L. B. Fu, and W. M. Zheng, Phys. Rev. A **63**, 011404(R) (2000); L. B. Fu, J. Liu, and S. G. Chen, Phys. Rev. A **65**, 021406 (2002); J. Chen and C. H. Nam, Phys. Rev. A **66**, 053415 (2002).

[4] V. L. B. de Jesus *et al.*, J. Electron Spectrosc. Relat. Phenom. **141**, 127 (2004); J. Phys. B **37**, L161 (2004).

[5] A. Becker, R. Dörner, and R. Moshammer, J. Phys. B **38**, S753 (2005).

[6] M. Weckenbrock *et al.*, J. Phys. B **34**, L449 (2001); Phys. Rev. Lett. **91**, 123004 (2003); Phys. Rev. Lett. **92**, 213002 (2004); E. Erimina *et al.*, J. Phys. B **36**, 3269 (2003); R. Moshammer *et al.*, J. Phys. B **36**, L113 (2003).

[7] B. Feuerstein *et al.*, Phys. Rev. Lett. **87**, 043003 (2001).

[8] R. Dörner *et al.*, Adv. At. Mol. Opt. Phys. **48**, 1 (2002).

[9] Th. Weber *et al.*, Nature (London) **405**, 658 (2000); Phys. Rev. Lett. **84**, 443 (2000); R. Moshammer *et al.*, Phys. Rev. Lett. **84**, 447 (2000).

[10] This is in contrast to the electron behavior in double ionization following single-photon absorption. See A. Emmanouilidou, T. Schneider, and J.-M. Rost, J. Phys. B **36**, 2717 (2003).

[11] R. Panfili, J. H. Eberly, and S. L. Haan, Opt. Express **8**, 431 (2001); R. Panfili, S. L. Haan, and J. H. Eberly, Phys. Rev. Lett. **89**, 113001 (2002); Phay J. Ho, R. Panfili, S. L. Haan, and J. H. Eberly, Phys. Rev. Lett. **94**, 093002 (2005).

[12] The one-electron aligned-electron model was introduced in J. Javanainen, J. H. Eberly, and Q. Su, Phys. Rev. A **38**, 3430 (1988); Q. Su and J. H. Eberly, Phys. Rev. A **44**, 5997 (1991). It was extended to two electrons in R. Grobe and J. H. Eberly, Phys. Rev. Lett. **68**, 2905 (1992).

[13] For a comprehensive recent review article, see A. Becker and F. H. M. Faisal, J. Phys. B **38**, R1 (2005).

[14] For this Letter, we start from a spatially radial Gaussian electron distribution and keep only trajectories that are compatible with our starting energy of -2.9035 a.u.. We apportion kinetic energy randomly between the two electrons in momentum space. Each electron is given zero angular momentum. Prior to the laser turn-on, we allow the ensemble to evolve for a time sufficient to achieve a stable distribution in phase space, which is then propagated from $t = 0$ when the laser is turned on. We have examined various initiating conditions to begin the phase-space filling procedure, including the quantum ground state, and have found that they all lead to very similar $t = 0$ distributions. All ensembles contain 400 000 two-electron trajectories.

[15] T. Brabec, M. Y. Ivanov, and P. B. Corkum, Phys. Rev. A **54**, R2551 (1996).

[16] In the present Letter we consider an electron to be ionized if either: (1) its kinetic energy and the potential energies of interactions with the nucleus and the other electron sum to greater than zero, or (2) the z component of the net force on the electron from the nucleus and laser points away from the nucleus with $|z| > 2.2$ a.u.. We have examined alternative definitions, and the conclusions of this Letter do not depend on our chosen definition.

[17] In our work we use a trapezoidal pulse, and the drift velocity is not affected by laser turn-off.

[18] See Phay J. Ho and J. H. Eberly, Phys. Rev. Lett. **97**, 083001 (2006).